Ocean Sci. Discuss., 11, 2173–2204, 2014
www.ocean-sci-discuss.net/11/2173/2014/
doi:10.5194/osd-11-2173-2014
© Author(s) 2014. CC Attribution 3.0 License.

Ocean Science
Discussions
Open Access

This discussion paper is/has been under review for the journal Ocean Science (OS).
Please refer to the corresponding final paper in OS if available.

Phytoplankton blooms on the western shelf of Tasmania: evidence of a highly productive ecosystem

J. Kämpf

School of the Environment, Flinders University, Adelaide, Australia

Received: 4 September 2014 – Accepted: 6 September 2014 – Published: 15 September 2014

Correspondence to: J. Kämpf (jochen.kaempf@flinders.edu.au)

Published by Copernicus Publications on behalf of the European Geosciences Union.

Abstract

Analyses of > 10 years of satellite-derived ocean-color data reveal the existence of a highly productive ecosystem on the west Tasmanian shelf. A closer event-based analysis indicates that the nutrient supply for this system has two different dynamical origins: (a) wind-driven coastal upwelling and (b) river plumes. During austral summer months, the west Tasmanian shelf forms a previously unknown upwelling center of the "Great South Australian Coastal Upwelling System", presumably injecting nutrient-rich water into western Bass Strait. Surprisingly, river discharges render the study region productive during other seasons of the year, except when nutrient-poor water of the South Australian Current reaches the region. Overall, the west Tasmanian shelf is more phytoplankton-productive than the long-known coastal upwelling along the Bonney Coast. The existence of phytoplankton blooms during the off-upwelling-season may explain the wintertime spawing aggregations of the blue grenadier (*Macruronus novaezelandiae*) and the associated regionally high abundance of Australian fur seals (*Arctocephalus pusillus doriferus*).

1 Introduction

Physical processes that enrich the euphotic zone with nutrients are principal agents of coastal phytoplankton blooms, including upwelling, storm-induced mixing, internal waves and river plumes. Except for the situation of coastal upwelling, vertical density stratification generally supports phytoplankton production, in particular when the surface mixed layer is relatively shallow and coincides with the euphotic zone.

The southern shelves of Australia host a large seasonal coastal upwelling system (Kämpf et al., 2004; Kämpf, 2010). In response to south-easterly coastal winds, upwelling events occur in austral summer months (December to April). This upwelling system, referred to as the "Great South Australian Coastal Upwelling System", consists of three upwelling centers (Fig. 1): the long-known Bonney Upwelling (Rochford, 1977; Lewis, 1981; Schahinger, 1987; Griffin et al., 1997), and upwelling centers off the southwest coast of Kangaroo Island and the southern tip of the Eyre Pensinula (Kämpf et al., 2004). The latter region plays a vital role in the life cycles of sardine (*Sardinops sagax*), anchovy (*Engraulis australis*), and southern bluefin tuna (*Thunnus maccoyii*) (Ward et al., 2006).

This study focusses on the western Tasmanian shelf. Throughout the year, the Zeehan Current runs southeastward confined to the shelf break along the continental shelf edge of western Bass Strait and western Tasmania (Cresswell, 2000). This current is the extension of the South Australian Current, which itself is the continuation of the Leeuwin Current (Ridgeway and Condie, 2004), but seasonally also entrains warm water formed during summer months on the shelves of the western Great Australian Bight (Herzfeld, 1997).

Currents within Bass Strait are created by tides, winds, incident continental shelf waves and density-driven flows (e.g., Sandery and Kämpf, 2005). Bass Strait is relatively shallow (~ 50–70 m) and main pathway of currents is generally eastward (Sandery and Kämpf, 2007). Prominent oceanographic features of Bass Strait are the existence of tidal mixing fronts on both sides of the strait (Sandery and Kämpf, 2005), and the wintertime formation of a density-driven overflow on the eastern side of the strait in vicinity of the Bass Canyon, known as the Bass Strait Cascade (Tomczak, 1985). Based on sparse field data, Gibbs and co-workers (Gibbs et al., 1986) concluded that nutrient levels in Bass Strait are overall low (< 1 µM in nitrate) except for the eastern edge where nutrient concentrations reach high levels (up to 7 µM in nitrate) in winter. According to these authors, chlorophyll *a* levels in Bass Strait are also generally low ($< 0.5\,\mathrm{mg\,m^{-3}}$) but show highest concentrations over the adjacent shelf, again in winter.

Earlier workers (Connolly and Von der Borch, 1967) postulated that upwelling of cold sub-Antarctic waters is the main reason for the occurrence of extensive temperate carbonates on the southern Australian shelves. Isotopic studies (e.g., Wass et al., 1970) validated this upwelling model for the formation of cold water carbonates. Interestingly, modern cold-water carbonate is also predominant sediment on the western Tasmanian shelf (Rao and Green, 1983). Isotope-based findings of Rao and Adibi (1992) demonstrate upwelling seawater as the main process responsible for the formation of carbonates in western Tasmania.

In austral winter, blue grenadier (*Macruronus novaezelandiae*) form spawning aggregations on the western Tasmanian shelf, being a key food source for Australian fur seals (*Arctocephalus pusillus doriferus*) (Hamer and Goldsworthy, 2006). Physical processes that drive the marine food chain in this region are not well understood.

Motivated by the findings of Rao and Adibi (1992) and Hamer and Goldsworthy (2006), this work explores phytoplankton blooms on the west Tasmanian shelf and their underlying physical processes.

2 Methodology

This work is based on satellite-derived spatial distributions of ocean colour (chlorophyll *a* concentration), coastal wind data, river discharges and, in part, sea surface temperature (SST). Ocean colour (SST) data are 8 day (5 day) composites.

This work focusses on two time periods. The first period extends from 1 January 1998 to 31 December 2000 (also used by Kämpf et al., 2004) and is adopted to establish initial evidence of the phytoplankton dynamics on the west Tasmanian shelf. This part of the study is based on the South East Fishery ocean movies (David Griffin, CSIRO, http://www.marine.csiro.au/~griffin/SEF/) using the SeaWiFS database (9 km resolution). Hereby it should be noted that of the 136 eight-day segments of chlorophyll *a* data, 35 segments (26 %) are missing for the western Tasmanian shelf due to cloud bias, mainly during austral winter/spring months.

The second, extended study period, 1 January 2005–31 March 2014, is used in an event-based statistical analysis of phytoplankton blooms is response to possible nutrient-supply events; that is, coastal upwelling events and/or river plumes. To this end, all relevant data are converted to 8 day segments in alignment with the ocean

cc BY

colour data, noting that SST data are not used in this event analysis. This part of the study uses NASA MODIS-aqua data (4 km resolution). For the west Tasmanian shelf, 90 (21 %) of the total of 425 eight-day segments are unusable due to cloud bias.

Wind data from the Cape Grim weather station (see Fig. 1) are used to calculate the classical upwelling index representative for the western Tasmanian shelf. This index is based on the theoretical offshore volume transport in the surface Ekman layer and is calculated from:

$$\mathrm{UI} = \frac{|\tau|}{\rho_o |f|} \cos(\alpha - \alpha'), \qquad (1)$$

where τ is wind stress, $\rho_o \approx 1026\,\mathrm{kg\,m^{-3}}$ is seawater density, $f \approx -0.9 \times 10^{-4}\,\mathrm{s^{-1}}$ is the value of the Coriolis parameter at 40° S, α is wind direction and α' is average coastline orientation, taken equivalent to 160° (based on the meteorological convention that 0° refers to northerly winds). Small variations of α' have little influence of the results (not shown). For initial comparison, we also calculated the upwelling index for the Bonney upwelling system for the period from 1 January 1998 to 31 December 2000.

River discharge data for the western coast of Tasmania are sparse. The only continuous time series of river discharge that the author could locate was that of the Davey River, located in south-western Tasmania (see Fig. 1). The flow is the Macquarie Harbour estuary, which is one of the largest freshwater sources on the western Tasmanian shelf, is unfortunately not routinely monitored. Without further evidence, the author postulates that the Davey River outflow can be taken as a proxy of that of other western Tasmanian rivers.

3 Results and discussion

3.1 Initial evidence based on SeaWiFS data (1998–2000)

Coastal upwelling on the southern shelves of Australia are associated with high-pressure weather systems that create southeasterly coastal winds (Kämpf et al., 2004). Due to their spatial scale and the geometry of Australia's coastline, such weather patterns can also initiate coastal upwelling on the western shelf of Tasmania. In early January 2000, for example, a high-pressure weather system developed centered over the South Australian Basin (Fig. 2). This high-pressure system became blocked by a low-pressure cell over Tasmania, triggering coast-parallel, upwelling-favorable winds along both Australia's southern shelves and the west coast of Tasmania. During this period, strong upwelling occurred in the upwelling centers of the southern shelf (Kämpf et al., 2004). During this event, chlorophyll *a* levels on the west Tasmanian shelf attained values of $\sim 3\,\mathrm{mg\,m^{-3}}$ being of the same order of magnitude as those observed in the upwelling center along the Bonney Coast (Fig. 3a). Upwelling-related negative SST anomalies can be identified in both regions (Fig. 3b). While the Bonney upwelling is pronounced with temperature anomalies of ~ 2–$3\,^{\circ}\mathrm{C}$, temperature anomalies on the western Tasmanian shelf are relatively difficult to distinguish from those in the ambient ocean which are of a similar range.

The time series of the upwelling indices for both regions (Fig. 4) reveals that, similar to the upwelling centers of Australia's southern shelves, coastal winds along the west coast of Tasmania are, on average, upwelling favorable during austral summer months (December–April). This indicates that both regions share similar wind-forced upwelling characteristics. Earlier work by Kämpf et al. (2004) has overlooked this feature.

While (running averages of) chlorophyll *a* levels off the Bonney Coast develop clear peaks during the austral summer upwelling season, chlorophyll *a* levels on the western shelf of Tasmania attain a complex temporal structure (Fig. 5a). In particular, large discrepancies in chlorophyll *a* levels between the regions occur in austral winter months.

In these instances, significant phytoplankton blooms appear on the west Tasmanian shelf.

The time series of SST (Fig. 5b) reveals intermittent "warming" periods from May to July; that is, during late austral autumn and early winter. These warming events, which are more pronounced along the Bonney Coast than on the western Tasmanian shelf, are associated with incursions of the South Australian Current (Fig. 6 shows an example). Being of shelf origin, this current has low nutrient content (e.g., Herzfeld, 1997) and its appearance in the study regions can be identified by marked reductions in chlorophyll *a* levels in each year of the time series (see Fig. 5a).

River discharges and associated river plumes are likely nutrient sources for the creation of phytoplankton blooms in the off-upwelling-season. Figure 7 shows selected events of coastal phytoplankton blooms on the western Tasmania shelf (and other shelf regions around Tasmania) in comparison with discharge rates of the Davey River. Given the large percentage of missing chlorophyll *a* data for austral winter/spring, no clear conclusions can be drawn here. The timing of some blooms on the west Tasmanian shelf seem to coincide with the onset of spring blooms in the western Tasman Sea, where chlorophyll *a* levels seasonally peaked in October at a level of 0.8 $\mathrm{mg\,m^{-3}}$ in the years 1998–2000 (Tilburg et al., 2002). It should be noted that the Bonney upwelling region is devoid of such spring blooms.

3.2 Detailed Analysis based on MODIS-aqua data (2005–2014)

Again, this data set confirms the pronounced annual periodicity of phytoplankton blooms in the Bonney upwelling region (Fig. 8a). Average peak chlorophyll *a* concentrations tend to slightly vary between the years, which reflects interannual variations of the frequency and intensity of individual upwelling events in this region. Middleton et al. (2007) speculated that this upwelling is strongly modulated by ENSO events, but the satellite data shown here are devoid of any dramatic interannual variability of upwelling intensity that could be linked to ENSO variability.

CC BY

In contrast to the Bonney upwelling, phytoplankton blooms on the west Tasmanian shelf occur in a highly irregular fashion and all year round (see Fig. 8a). Overall, blooms in both regions attain similar peak values of up to $3\,\mathrm{mg\,m^{-3}}$. The upwelling index for the west Tasmanian shelf generally attains positive values for austral summer months (Fig. 8b). In some years, this index indicates brief upwelling events outside the summer season. For instance, the year 2007 had such an event in June, and several of the years (e.g. 2005 and 2013) had early upwelling-favourable wind events in November, being mirrored by individual phytoplankton blooms (see Fig. 8a). On the other hand, the upwelling index also indicates events of strong downwelling-favourable winds, such as in August 2009.

Overall, the discharge from the Davey River tends to peak in austral winter/spring with markedly reduced flows during austral summer months (Fig. 8c). An exception is the year break of 2005/06 which had a relatively strong riverine discharge occurring in December/January.

For completeness, the author also included a time series of wind stress (Fig. 8d), given that strong storms have the abilitity to modify phytoplankton blooms via changes in the mixed-layer depth and potential entrainment of nutrient-rich water from below. On the other hand, storms can also "mix away" any vertical structure of phytoplankton concentrations, thereby removing the surface appearance of a phytoplankton bloom. For instance, the existence of relatively strong winds ($\sim 2.5\,\mathrm{Pa}$) in January 2007 might explain relatively low surface chlorophyll *a* levels in west Tasmanian coastal water although these winds were upwelling favourable. Similarly, despite strong river discharge in August–September 2009, strong wind stresses ($> 2.5\,\mathrm{Pa}$) coexisted with relatively low chlorophyll *a* levels (accompanied by a downwelling-favourable wind direction). Given the relatively small number of stronger storm events occuring during the observation period, however, the wind-stress influence on the dynamics of phytoplankton bloom on the western Tasmanian shelf remains inconclusive. It should be noted that periods of 3–7 days of relaxed winds after a brief upwelling event are deemed optimal

Title Page
Abstract | Introduction
Conclusions | References
Tables | Figures
◀| |▶
◀ ▶
Back | Close
Full Screen / Esc
Printer-friendly Version
Interactive Discussion

for phytoplankton accumulation (Wilkenson et al., 2006). This relaxation effect is not explored in the context of this work.

Despite relatively large data gaps due to cloud bias, several phytoplankton blooms that occurred on the west Tasmanian shelf in the period from 2005 to 2014 can be illustrated with spatial chlorophyll *a* distributions (Fig. 9). Some phytoplankton blooms can hereby be affiliated with wind-driven coastal upwelling events (e.g. 10 March 2005, 10 March 2009, 12 October 2010), whereas other events can be linked to increased river discharge (e.g. 24 July 2006, 24 July 2008, 19 October 2008, 5 May 2013).

3.3 Event Analysis (2005–2014)

When using window-averaged data, a standard cross-correlation analysis between upwelling index, chlorophyll *a* concentrations and river discharges does not give satisfactory results. Overall, the resultant correlation coefficients are insignificantly small and strongly biased by data smoothing and interpolation (see Fig. 10 to compare smoothed and original 8-day composite data). Instead of this, statistically more relevent information can be derived from an event-based analysis, whereby all relevant data are averaged onto 8-day data segments, with each data segment being defined as an individual event. The underlying assumption is that phytoplankton blooms follow within ~ 3–7 days after a nutrient-supply event. This implies that there is a relatively high probability that physical events (upwelling or appearance of river plumes) trigger a bloom within the timescale (8 days) of a data segment. This assumption is consistent with observational evidence (Wilkerson et al., 2006).

This approach, for instance, returns histograms of chlorophyll *a* ranges for the study region in comparison with the Bonney upwelling region (Fig. 11). High levels $> 2\,\mathrm{mg\,m^{-3}}$ can be associated with phytoplankton blooms. Such levels are found off the Bonney Coast for ~ 7.8 % of time, which is equivalent to roughly 28 days per year. In the study region, high chlorophyll *a* levels $> 2\,\mathrm{mg\,m^{-3}}$ occurred 27 % of time, which corresponds to around 100 days per year. Hence, the west Tasmanian shelf is considerably more productive than the Bonney upwelling region.

CC BY

A quick analysis of other relevant parameter reveals a slightly higher frequency of upwelling-favourable (~ 60 % of time) than downwelling-favourable wind conditions (Fig. 12a). Despite its irregularity, the discharge of the Davey River is relatively weak ($< 25\,\mathrm{m^3\,s^{-1}}$) for ~ 42 % of time corresponding to ~ 150 days per annum, whereas strong discharges ($> 75\,\mathrm{m^3\,s^{-1}}$) occur for ~ 17 % of time, being equivalent to ~ 60 days per annum (Fig. 12b). When averaged on eight-day data segments, most (~ 59 % of time) wind events attain wind stresses in a range of 0.1 to 0.2 Pa, whereas strong storm events of wind stresses > 0.3 Pa are relatively rare (< 6 % of time).

When grouping data segments into different intervals of upwelling index and river discharge, the largest number of records exist for large values of the upwelling index $> 0.25\,\mathrm{m^2\,s^{-1}}$ in the presence of relatively low river discharge $< 50\,\mathrm{m^3\,s^{-1}}$ (Table 1). This criterion returns 143 of the 335 valid events (~ 42.7 %). On the other hand, a relatively large number of valid data segments exists for stronger river discharges $> 50\,\mathrm{m^3\,s^{-1}}$ and negative values of the upwelling index, returning 57 events (~ 17 %). This criterion correponds to periods of enhanced river discharges, typically occuring during austral winter and spring months (see Fig. 8c). The other intervals considered have statistically satisfactory population sizes between 9 and 24 events.

While some data are missing due to cloud bias for all intervals of upwelling index and river discharge considered, the criterion of stronger river discharges $> 50\,\mathrm{m^3\,s^{-1}}$ and negative values of the upwelling index < –0.25 stand out with 34 of the total of 90 missing events (~ 38 %) (Table 2). Most of these cloud events tend to occur during austral winter months (results not shown).

Consistent with the aforementioned weak cross-correlations between parameters, average chlorophyll *a* concentrations are of the same order of magnitude for all parameter intervals considered (Fig. 13a). This implies, for instance, that stronger upwelling-favourable winds do not always create phytoplankton blooms.

With a focus on events of phytoplankton blooms of chlorophyll *a* concentrations $> 2\,\mathrm{mg\,m^{-3}}$ the outcome is vastly different (Fig. 13b). Here, the by far largest number of blooms occurs for upwelling favourable winds ($\mathrm{UI} > 0.25\,\mathrm{m^2\,s^{-1}}$) yielding a total of 47 of

94 events (50 %). More than half (26) of these events occur during low river discharges, which is characteristic of the austral summer season. Hence, these events can be attributed to the classical wind-driven upwelling mechanism. On the other hand, there are a total of 25 phytoplankton blooms developping during periods of stronger river discharges ($> 50\,\mathrm{m^3\,s^{-1}}$). A relatively large number (13, or ~ 60 %) of these blooms developed in the presence of downwelling-favourable winds. These events can be attributed to nutrient supply via river plumes. Overall, events of either $\mathrm{UI} > 0.25\,\mathrm{m^2\,s^{-1}}$ or river discharges $> 50\,\mathrm{m^3\,s^{-1}}$ explain ~ 70 % of the identified phytoplankton blooms. Some of the remainder 30 % of events are associated with “phase shifts”, i.e. a stronger upwelling event or river discharge event occurred in the preceding data segment. Other plankton blooms are caused by river discharges in the upper range of the 25–50 $\mathrm{m^3\,s^{-1}}$ interval. Hence, most of the identified phytoplankton blooms can be linked either to upwelling events or river plumes.

While the outcome based on phytoplankton blooms gives conclusive results, there are a total of 180 events with $\mathrm{UI} > 0.25\,\mathrm{m^2\,s^{-1}}$ during the study period of which only 47 (26 %) triggered a phytoplankton bloom with chlorophyll *a* concentrations exceeding $2\,\mathrm{mg\,m^{-3}}$. Another 14 events (8 %) follow when accounting for the upwelling index from the preceding data segment. Similarly, there are 139 events of river discharges $> 50\,\mathrm{m^3\,s^{-1}}$, whereby only 25 (18 %) can be linked to phytoplankton blooms. Another 26 (19 %) events follow when accouting for river-discharge events that occurred in preceding data segments. Overall, only 34 % of such events of upwelling-favourable winds and 37 % of river-discharge events created phytoplankton blooms.

A number of possible processes could explain these missing phytoplankton blooms including (a) the lack of sufficiently long periods of relaxed wind after upwelling events (Wilkerson et al., 2006), (b) preceding downwelling periods that create a southward geostrophic coastal current and offshore transport in the bottom Ekman layer that, due to inertia effects, resist subsequent wind changes, (c) incursions of nutrient-low water from the South Australian Current, and (d) nutrient limitation. A more detailed analysis of possible causes of the missing blooms is beyond the scope of this study.

In order to compare total phytoplankton productivity between the Bonney upwelling system and the west Tasmanian shelf, we assume that (a) the spatial extent of their productivity zones is similar, and (b) eight-day composite values of chlorophyll *a* concentration are proportional to the amount of phytoplankton formed during the eight-day period. This assumption gives an estimate of ~ 530 mg (per unit volume) in total production for the west Tasmanian shelf over the entire study period (Fig. 14). This exceeds total production of the Bonney upwelling region by more than 50 %. Given the relatively large fraction of missing winter/autumn data, the true productivity may be even higher. In contrast to the Bonney upwelling system, substantial production occurs during the austral winter/spring months on the west Tasmanian shelf.

Finally, it should be stressed that the coastal currents involved in river plumes and upwelling distribute nutrients differently along the shelf. Coastal upwelling jets tend to move nutrient-rich water right-bounded by the coast; i.e., northward along the coast and possibly into western Bass Strait (Fig. 15a gives an example). On the other hand, river plumes tend to disperse (different types and compositions) of nutrients left-bounded by the coast; i.e. southward along the coast (Fig. 15b gives an example).

4 Conclusions

A detailed analysis of satellite-derived ocean colour data for the periods 1998–2000 and 2005–2014 suggest that the west Tasmanian shelf accommodates a highly productive ecosystem, in which phytoplankton blooms occur irregularly all year round. In austral summer, this region forms another upwelling center of the Great South Australian Coastal Upwelling System. The addition of this newly discovered center makes this system one of the largest (total spatial extension ~ 1500 km) seasonal coastal upwelling systems on Earth.

The accuracy of satellite radar altimeter sea surface height measurement degrades in coastal region (Roesler et al., 2013) and cannot be used to identify upwelling jets on the western Tasmanian shelf. Nevertheless, classical upwelling theory suggests the existence of such jets dispersing nutrient-rich water northward along the shelf and possible into western Bass Strait. This advective process would explain elevated chlorophyll *a* levels in western Bass Strait – a typical feature of the region during austral summer months (see Figs. 3a and 15a). As such, upwelling on the western Tasmanian shelf presumably constitutes an important nutrient source for Bass Strait.

In austral winter and spring months, river discharges and associated river plumes continue to fertilize the coastal ocean on the west Tasmania shelf, which may explain the high abundance of blue grenadier and Australian fur seals in the region. Findings indicate that the only clearly definable periods in which phytoplankton production markedly decreases is when nutrient-poor waters of the South Australian Current appear in the region. Overall, the west Tasmanian shelf appears to be $> 50\,\%$ more productive than the long-known Bonney upwelling region.

Acknowledgements. The author thanks Paul Sandery (Bureau of Meteorology, Australia) for the provision of Cape Grim wind data. This work has not received external funding. The author declares that there is no conflict of interests regarding the publication of this paper.

References

Conolly, J. R. and Von der Borch, C. C.: Sedimentation and physiography of the sea floor south of Australia, Sediment. Geol., 1, 181–220, doi:10.1016/0037-0738(67)90059-0, 1967.

Cresswell, G.: Currents of the continental shelf and upper slope of Tasmania, Papers and Proceedings of the Royal Society of Tasmania, 133, 21–30, 2000.

Gibbs, C. F., Tomczak, M., and Longmore, A. R.: The nutrient regime of Bass Strait, Aust. J. Mar. Fresh. Res., 37, 451–466, 1986.

Griffin, D. A., Thompson, P. A., Bax, N. J., and Hallegraeff, G. M.: The 1995 mass mortality of pilchards: no role found for physical or biological oceanographic factors in Australia, Aust. J. Mar. Fresh. Res., 48, 27–58, 1997.

Hamer, D. J. and Goldsworthy, S. D.: Seal-fishery interactions: identifying the environmental and operational aspects of a trawl fishery that contribute to by-catch and mortality of Australian fur seals (*Arctocephalus pusillus doriferus*), Biol. Conserv., 130, 517–529, 2006.

cc BY

Herzfeld, M.: The annual cycle of sea surface temperature in the Great Australian Bight, Prog. Oceanogr., 39, 1–27, doi:10.1016/S0079-6611(97)00010-4, 1997.

Kämpf, J.: On the preconditioning of coastal upwelling in the eastern Great Australian Bight, J. Geophys. Res.-Oceans, 115, C12071, doi:10.1029/2010JC006294, 2010.

Kämpf, J., Doubell, M., Griffin, D., Matthews, R. L., and Ward, T. M.: Evidence of a large seasonal coastal upwelling system along the southern shelf of Australia, Geophys. Res. Lett., 31, L09310, doi:10.1029/2003GL019221, 2004.

Lewis, R. K.: Seasonal upwelling along the southeastern coastline of South Australia, Aust. J. Mar. Fresh. Res., 32, 843–854, 1981.

Middleton J. F., Arthur, C., van Ruth, P., Ward, T., McClean, J., Maltrud, M., Gill, P., and Middleton, S.: ENSO effects and upwelling along Australia's southern shelves, J. Phys. Oceanogr., 37, 2458–2477, 2007.

Rao, C. P. and Adabi, M. H.: Carbonate minerals, major and minor elements and oxygen and carbon isotopes and their variation with water depth in cool, temperate carbonates, western Tasmania, Australia, Mar. Geol., 103, 249–272, doi:10.1016/0025-3227(92)90019-E, 1992.

Rao, C. P. and Green, D. C.: Oxygen- and carbon-isotope composition of cold shallow-marine carbonates of Tasmania, Australia, Mar. Geol., 53, 117–129, doi:10.1016/0025-3227(83)90037-3, 1983.

Ridgway, K. R. and Condie, S. A.: The 5500-km-long boundary flow off western and southern Australia, J. Geophys. Res.-Oceans, 109, c04017, doi:10.1029/2003JC001921, 2004.

Rochford, D. J.: A review of possible upwelling situation off Port MacDonald, South Australia, CSIRO Australian Division Oceanography Report No. 81, 4 pp., 1977.

Roesler, C. J., Emery, W. J., and Kim, S. Y.: Evaluating the use of high-frequency radar coastal currents to correct satellite altimetry, J. Geophys. Res.-Oceans, 118, 3240–3259, doi:10.1002/jgrc.20220, 2013.

Sandery, P. A. and Kämpf, J.: Winter-spring flushing of bass strait, south-eastern Australia: a numerical modelling study, Est. Coast. Shelf Sci., 63, 23–31, doi:10.1016/j.ecss.2004.10.009, 2005.

Sandery, P. A. and Kämpf, J.: Transport timescales for identifying seasonal variation in Bass Strait, south-eastern Australia, Estuar. Coast. Shelf S., 74, 684–696, doi:10.1016/j.ecss.2007.05.011, 2007.

Schahinger, R. B.: Structure of coastal upwelling events observed off the southern coast of South Australia during Feb 1983–April 1984, Aust. J. Mar. Fresh. Res., 38, 439–459, 1987.

CC BY

Tilburg, C. E., Subrahmanyam, B., and O'Brien, J. J.: Ocean color variability in the Tasman Sea, Geophys. Res. Lett., 29, 125-1–125-4, doi:10.1029/2001GL014071, 2002.

Tomczak, M.: The Bass Strait water cascade during winter 1981, Cont. Shelf Res., 2, 55–87, 1985.

Ward, T. M., McLeay, L. J., Dimmlich, W., Rogers, A., McClatchie, S., Matthews, R. L., Kämpf, J., and Van Ruth, P. D.: Pelagic ecology of a northern boundary current system: effects of upwelling on the production and distribution of sardine (Sardinops sagax), anchovy (Engraulis australis) and southern bluefin tuna (Thunnus maccoyii) in the Great Australian Bight, Fishery Oceanogr., 15, 191–207, doi:10.1111/j.1365-2419.2006.00353.x, 2006.

Wass, R. E., Connolly, R. J., and MacIntyre, R. J.: Bryozoan carbonates and sand continuous along southern Australia, Mar. Geol., 9, 63–73, doi:10.1016/0025-3227(70)90080-0, 1970.

Wilkerson, F. P., Lassiter, A. M., Dugdale, R. C., Marchi, A., and Hogue, V. E.: The phytoplankton bloom response to wind events and upwelled nutrients during the CoOP WEST study, Deep-Sea Res. Pt. II, 53, 3023–3048, 2006.

cc BY

Table 1. Number of valid events of the time series (1 January 2005 to 31 March 2014) grouped according to different intervals of Upwelling Index (UI) and River Discharge (*R*).

↓ R (m^3 s^{-1}) UI (m^2 s^{-1}) →	$< -1/4$	$-1/4$ to 0	0 to $+1/4$	$> +1/4$	all UI
< 25	9	21	24	107	161
25 to 50	15	12	22	36	85
> 50	47	10	13	19	89
all *R*	71	43	59	162	$\Sigma = 335$

Table 2. Number of missing events of the time series (1 January 2005 to 31 March 2014) grouped according to different intervals of Upwelling Index (UI) and River Discharge (R).

↓ R ($\mathrm{m^3\,s^{-1}}$) UI ($\mathrm{m^2\,s^{-1}}$) →	$< -1/4$	$-1/4$ to 0	0 to $+1/4$	$> +1/4$	all UI
< 25	3	2	5	6	16
25 to 50	5	6	6	7	24
> 50	34	4	7	5	50
all R	42	12	18	18	$\Sigma = 90$

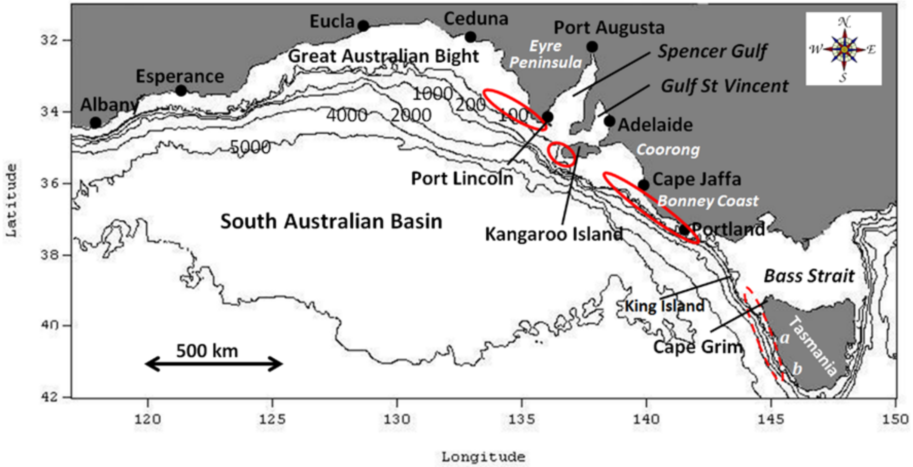

Figure 1. The geography of Australia's southern shelves. Isobath depths are in meters. Solid-line ellipses display known locations of coastal upwelling centers. The dashed-line ellipse highlights the region investigated in this paper. Letters a and b show the locations of the mouths of Macquarie Harbour and Davey River.

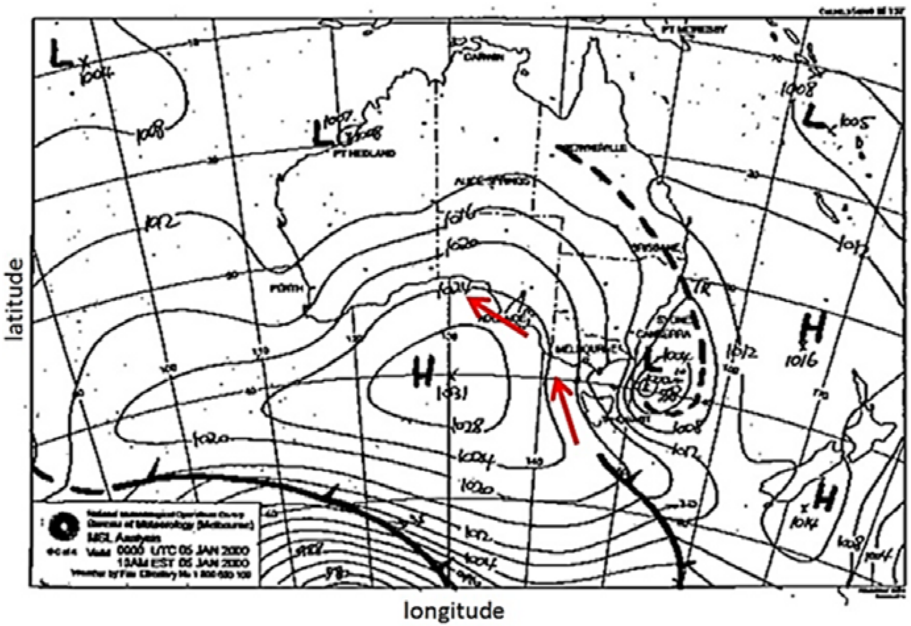

Figure 2. Mean sea level pressure for 6 January 2000, courtesy of the Bureau of Meteorology (Australia). Arrows indicate upwelling-favorable coastal winds, influenced by a blocking, low-pressure cell over Tasmania.

CC BY

OSD
11, 2173–2204, 2014

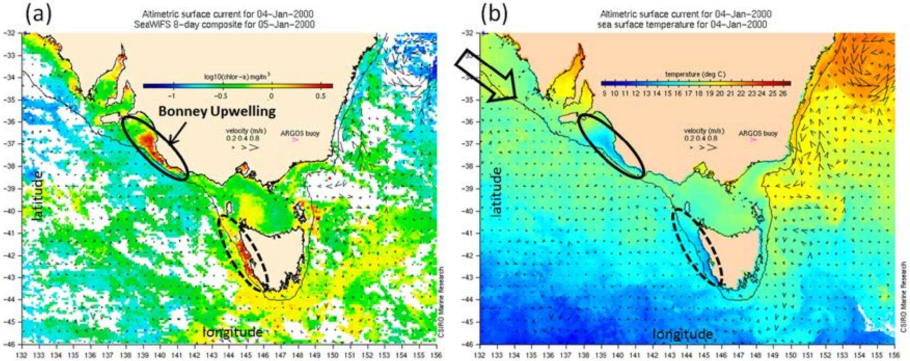

Figure 3. Occurrence of a pronounced coastal upwelling event in early January of 2000, evident in satellite-derived distributions of **(a)** chlorophyll *a* and **(b)** sea surface temperature. White regions in panel **(a)** are missing data due to clouds. The large arrow in panel **(b)** indicates the pathway of the South Australian Current. Data source: South East Fishery ocean movies, David Griffin, CSIRO, http://www.marine.csiro.au/~griffin/SEF/.

Title Page
Abstract Introduction
Conclusions References
Tables Figures
◀| |▶
◀ ▶
Back Close
Full Screen / Esc
Printer-friendly Version
Interactive Discussion

Title Page
Abstract
Introduction
Conclusions
References
Tables
Figures
◀|
|▶
◀
▶
Back
Close
Full Screen / Esc
Printer-friendly Version
Interactive Discussion

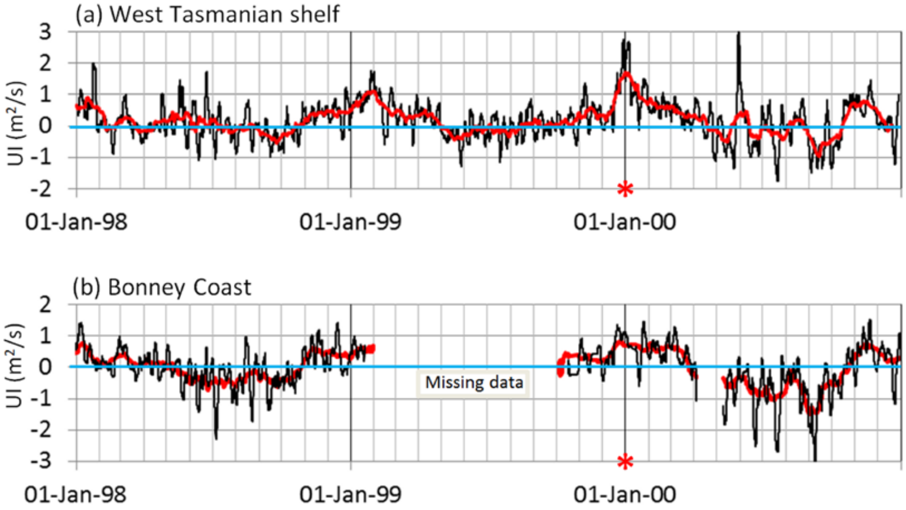

Figure 4. Time series (1 January 1998–31 December 2000) of the upwelling index ($m^2\ s^{-1}$) for **(a)** the west Tasmanian shelf and **(b)** the Bonney Coast. Thin, black (thick, red) curves are 4 day (20 day) moving averages. Stars highlight an upwelling events in the early January 2000, corresponding to the spatial distributions shown in in Fig. 3. Data source: Bureau of Meteorology, Australia.

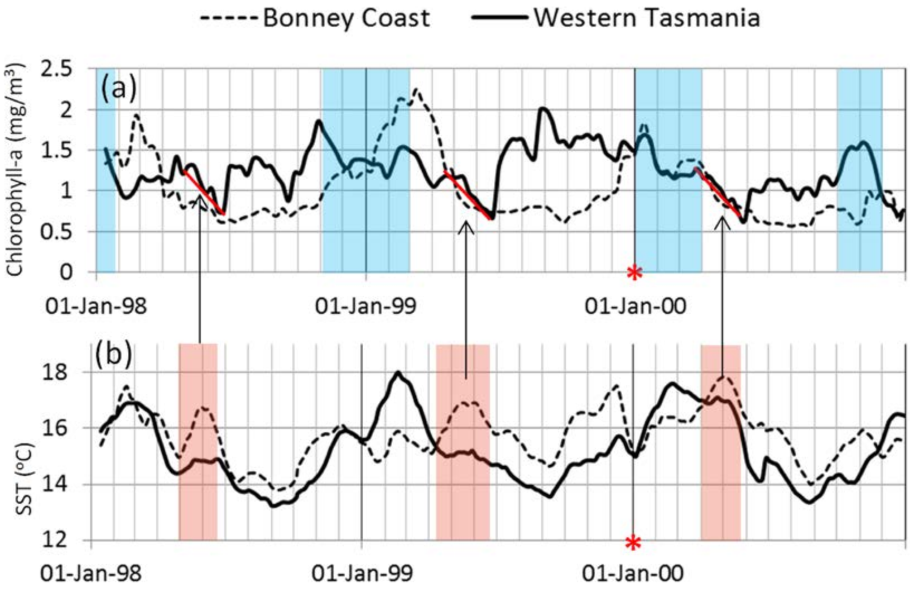

Figure 5. Time series (1 January 1998–31 December 2000) of satellite-derived data of **(a)** chlorophyll *a* (mg m^{-3}) and **(b)** sea surface temperature (SST, °C) for the Bonney Coast and the west Tasmanian shelf, applying running averages over 24 days for ocean colour and 20 days for SST. Shaded areas of panel **(a)** denote periods of upwelling-favorable coastal winds (see Fig. 4). Shaded areas in panel **(b)** denote temperature increases due to incursions of the nutrient-poor South Australian Current that can be associated with periods of decreasing chlorophyll *a* concentrations in panel **(a)**. Stars highlight an upwelling events in the early January 2000, corresponding to the spatial distributions shown in in Fig. 3. Data source: South East Fishery ocean movies, David Griffin, CSIRO, http://www.marine.csiro.au/~griffin/SEF/.

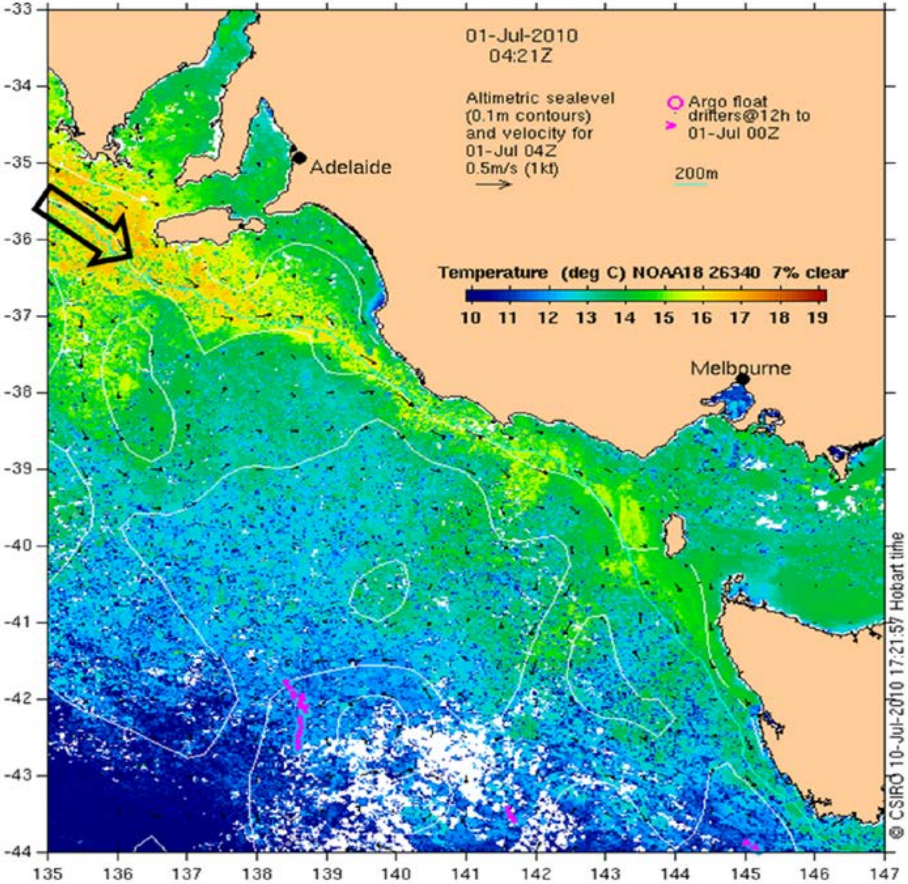

Figure 6. An example of the inflow of warm, nutrient-low South Australian Current that typically appears along the Bonney Coast and on the western Tasmanian shelf between May and July every year. Data source: Integrated Marine Observing System (IMOS), http://oceancurrent.imos.org.au/Adelaide/2010/2010070104.html.

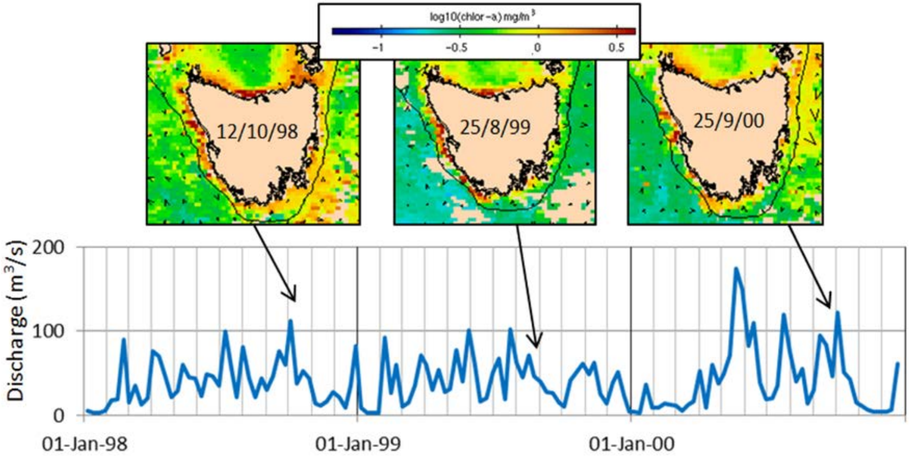

Figure 7. Eight-day averages of freshwater discharge from the Davey River (see Fig. 1 for approximate location) for the period of 1 January 1998–31 December 2000 and selected satellite-derived chlorophyll *a* distributions (8 day composites). Source of river data: Water Information System of Tasmania, http://wrt.tas.gov.au/wist/ui. Source of satellite data: South East Fishery ocean movies, David Griffin, CSIRO, http://www.marine.csiro.au/~griffin/SEF/. Logarithmic values of −0.5, 0 and 0.5 correspond to chlorophyll *a* concentations of ~ 0.3, 1, and 3 mg m^{-3}, respectively.

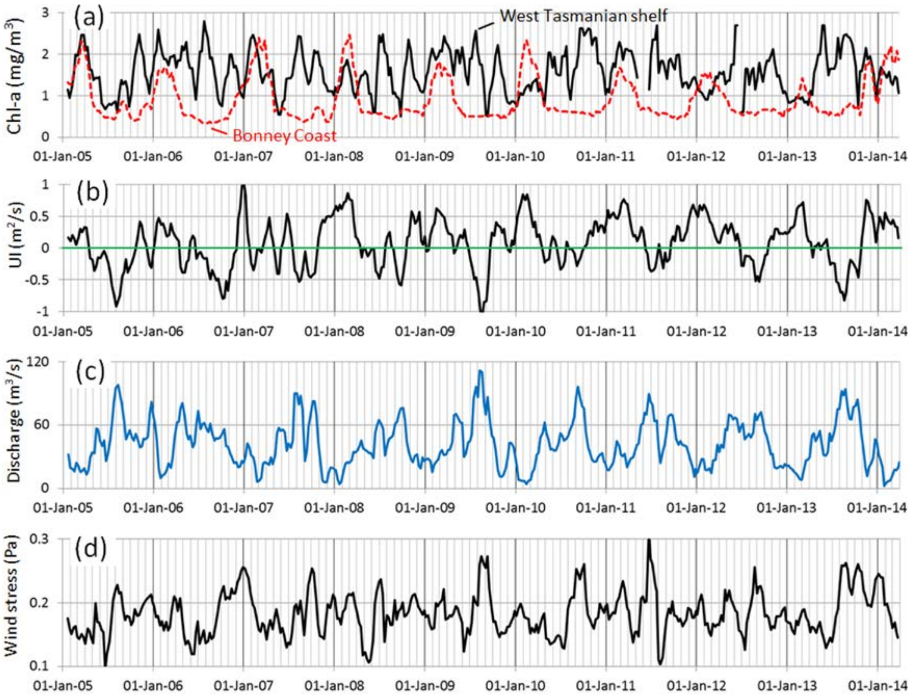

Figure 8. Time series (1 January 2005–31 March 2014) of **(a)** chlorophyll *a* concentration, **(b)** upwelling index, **(c)** freshwater discharge from the Davey River, and **(d)** wind stress. Data were first converted to 8 day segments and then smoothed with a running average over three segments. For comparison, panel **(a)** includes data for the Bonney upwelling. Data sources: NASA, Bureau of Meteorology (Australia), and Water Information System of Tasmania.

cc BY

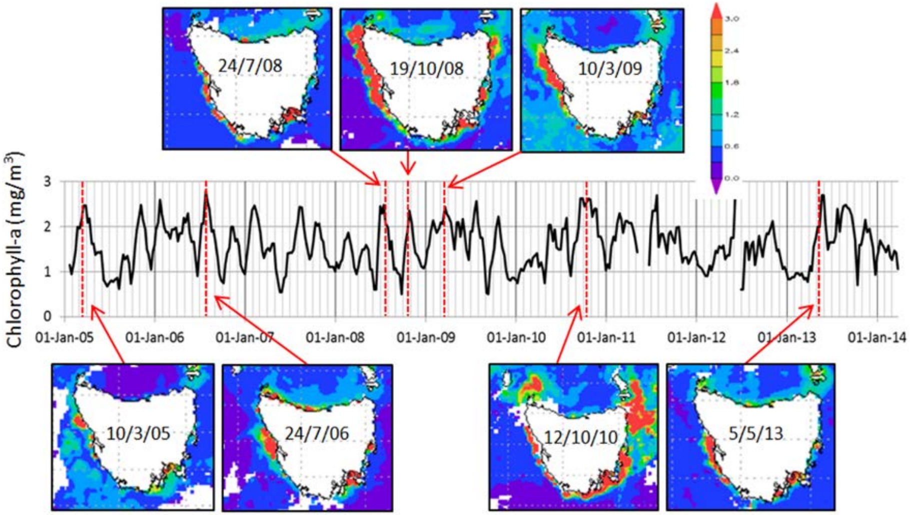

Figure 9. Time series (1 January 2005–31 March 2014) of chlorophyll *a* concentration (same as black curve in Fig. 8a) and selected satellite-derived 8 day composites (data source: NASA, http://disc.sci.gsfc.nasa.gov/giovanni).

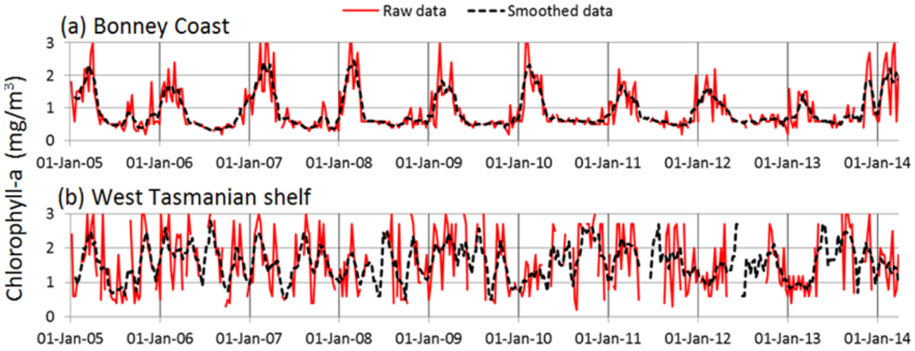

Figure 10. Time series (1 January 2005–31 March 2014) of chlorophyll *a* data for **(a)** the Bonney Coast and **(b)** the west Tasmanian shelf. Solid, red lines show original values derived from 8 day composites with missing data left blank. Dashed, black lines display smoothed data, also shown in Fig. 8a.

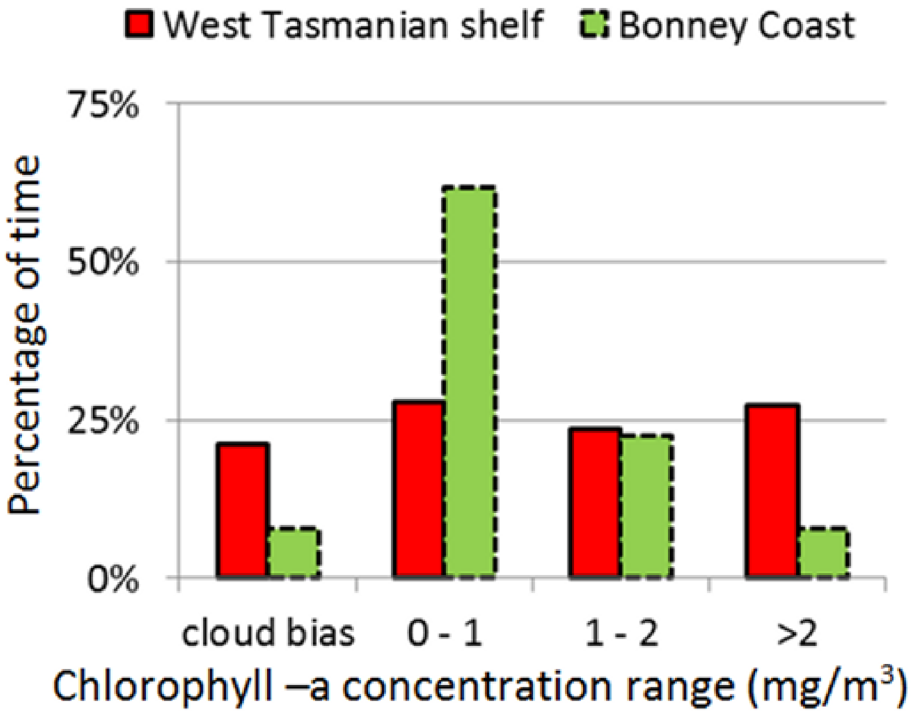

Figure 11. Event analysis. Histogram of 8 day segments during the period from 1 January 2005 to 31 March 2014 that fall within certain ranges of chlorophyll *a* concentrations. “Cloud bias” refers to missing data.

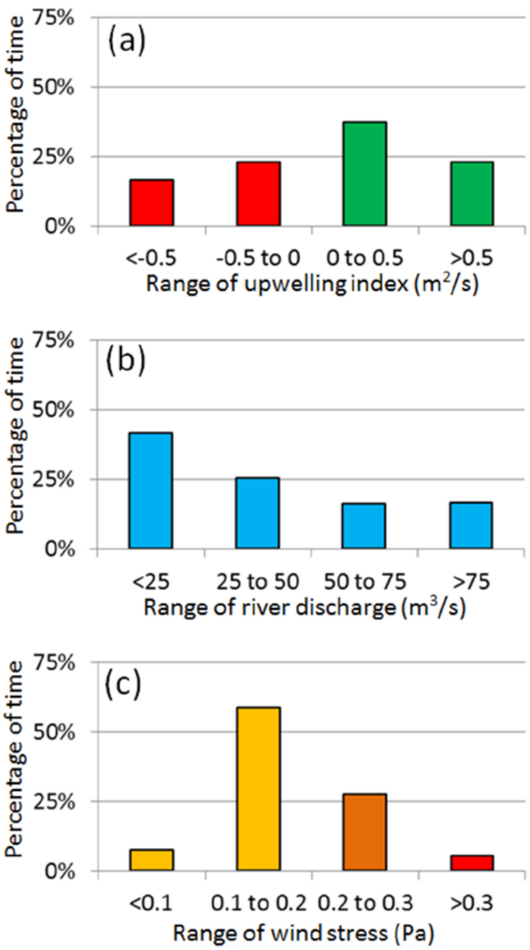

Figure 12. Same as Fig. 11, but displaying the event statistics for **(a)** upwelling index, **(b)** discharge from the Davey River, and **(c)** magnitude of the wind stress.

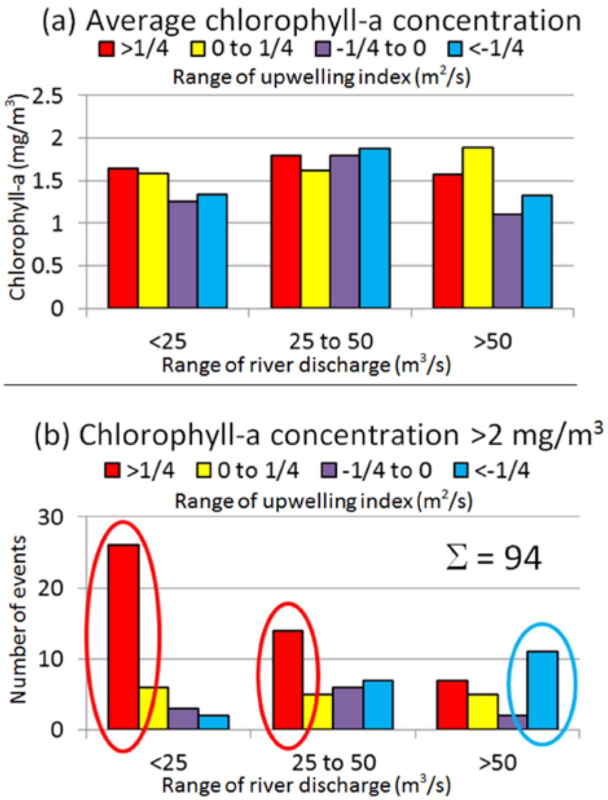

Figure 13. Event analysis of the time series from 1 January 2005 to 31 March 2014. **(a)** Average chlorophyll *a* value for 8 day segments that fall into certain intervals of upwelling index and discharge from the Davey River. The total number of segments is 335. **(b)** Number of data segments of a chlorophyll *a* concentration $> 2\,\mathrm{mg\,m^{-3}}$, being grouped as in panel **(a)**. A total of 94 data segments satisfy this condition. The ellipses highlight the most frequent events in each interval of river discharges considered.

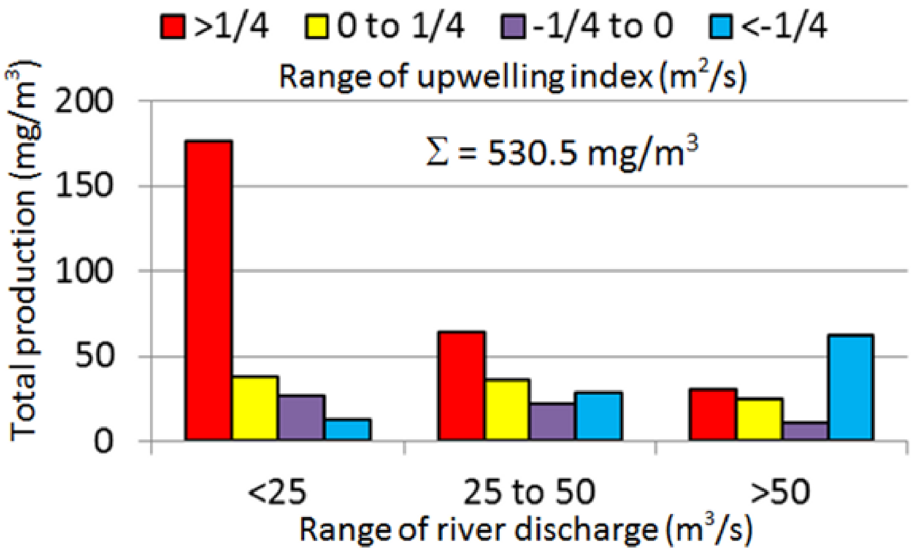

Figure 14. Same as Fig. 13a, but showing total production ($\mathrm{mg\,m^{-3}}$) (see text for definition). In comparison, the Bonney upwelling attains a total production of 361 $\mathrm{mg\,m^{-3}}$.

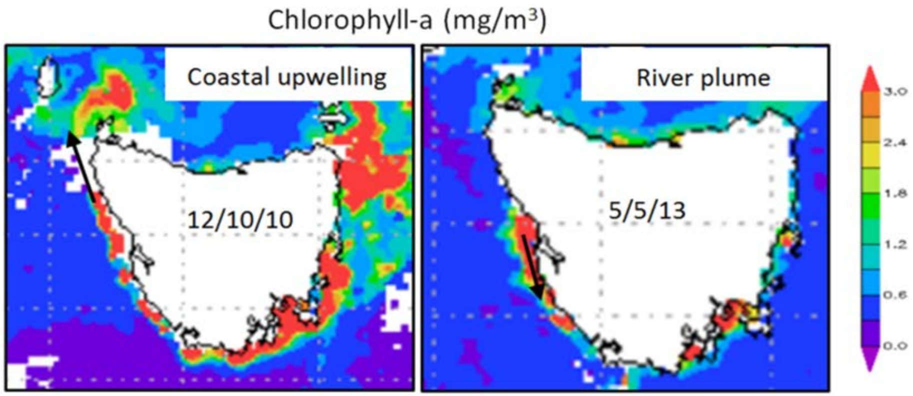

Figure 15. Examples of satellite-derived chlorophyll *a* distributions being characteristic of **(a)** a wind-driven coastal upwelling event, and **(b)** a river plume. The arrows indicate dominant flow directions.

Title Page
Abstract
Introduction
Conclusions
References
Tables
Figures
◄|
|►
◄
►
Back
Close
Full Screen / Esc
Printer-friendly Version
Interactive Discussion